Science of the Total Environment 566–567 (2016) 1254–1267

Contents lists available at ScienceDirect

Science of the Total Environment

journal homepage: www.elsevier.com/locate/scitotenv

Distribution, sources and ecological risk assessment of polycyclic aromatic hydrocarbons in water and sediments from Tiber River and estuary, Italy

Paolo Montuori [a,*], Sara Aurino [a], Fatima Garzonio [a], Pasquale Sarnacchiaro [b], Antonio Nardone [a], Maria Triassi [a]

[a] Department of Public Health, University Federico II, Via Sergio Pansini no 5, 80131 Naples, Italy
[b] Department of Economics, University Unitelma Sapienza, Viale Regina Elena no 295, 00161 Rome, Italy

HIGHLIGHTS

- Light PAHs were mostly detected in water and heavy PAHs appeared mostly in sediment.
- Pyrolytic PAHs sources are predominant.
- PAHs concentrations were remarkably high at a site just before the fork of the river.
- PAHs levels in sediment were compared SQGs.
- TEQ_{PAHs} suggest potentially low carcinogenicity of PAHs exposure in Tiber River and Estuary.

GRAPHICAL ABSTRACT

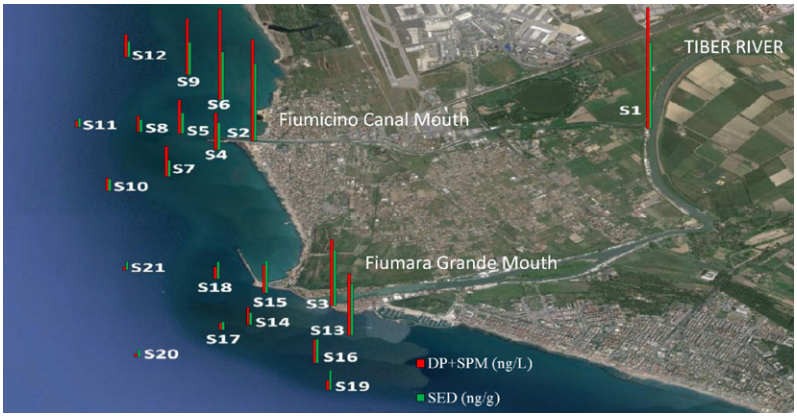

ARTICLE INFO

Article history:
Received 15 April 2016
Received in revised form 25 May 2016
Accepted 26 May 2016
Available online 2 June 2016

Editor: D. Barcelo

Keywords:
Tiber river
Polycyclic aromatic hydrocarbons
Source
Contaminant loads
Risk assessment
Toxic equivalent quantity (TEQ)

ABSTRACT

The concentration, source and ecological risk of polycyclic aromatic hydrocarbons (PAHs) in the Tiber River and its environmental impact on the Tyrrhenian Sea (Central Mediterranean Sea) were estimated. The 16 priority PAHs were determined in the water dissolved phase (DP), suspended particulate matter (SPM) and sediments collected from 21 sites in four different seasons. Total concentrations of PAHs ranged from 10.3 to 951.6 ng L^{-1} and from 36.2 to 545.6 ng g^{-1} in water (sum of DP and SPM) and in sediment samples, respectively. The compositions of PAHs showed that 2- to 4-ring PAHs were abundant in DP, 4- to 6-ring PAHs were predominant in SPM samples, and 4- to 5-ring PAHs were abundant in sediments. The diagnostic ratio analysis indicated that the PAHs mainly had a pyrolytic source. The toxic equivalent concentration of carcinogenic PAHs was 45.3 ngTEQ g^{-1}, suggesting low carcinogenic risk for Tiber River. Total PAHs loads into the sea were calculated in about 3161.7 kg $year^{-1}$ showing that this river is one of the main contribution sources of these contaminants to the Tyrrhenian Sea.

* Corresponding author.
E-mail address: pmontuor@unina.it (P. Montuori).

http://dx.doi.org/10.1016/j.scitotenv.2016.05.183
0048-9697/

1. Introduction

Polycyclic aromatic hydrocarbons (PAHs) are a widespread class of environmental pollutants (Moeckel et al., 2013; Li et al., 2015a; Santana et al., 2015; Zhao et al., 2015). Due to their persistent, toxic, genotoxic and carcinogenic characteristics and potential human health risk, PAHs distribution and source in the environment have attracted much attention (Song et al., 2013; Bai et al., 2014; Siemers et al., 2015; Yu et al., 2015; Sarria-Villa et al., 2016). Numerous epidemiological studies have demonstrated a correlation between PAHs exposure and cancer incidence for various human tissues (Cirillo et al., 2006; Lv et al., 2014; Zhi et al., 2015). For this reason, 16 PAHs were designated as priority pollutants by the United States Environmental Protection Agency (USEPA) and seven of them were designated as potentially carcinogenic pollutants to humans, according to the International Agency for Research on Cancer (Zheng et al., 2016).

PAHs can originate from incomplete combustion of organic matter, dry and wet deposition, wastewater discharge, oil pollution and road runoff. Due to their physicochemical properties, PAHs tend to interact to different extent with air, water, soil/sediment and biota (Guo et al., 2009; Zhao et al., 2014; Pérez-Fernández et al., 2015). In marine and freshwater ecosystems, PAHs are absorbed onto particulate matter and accumulate in sediments. Sediments, the primary reservoir for hydrophobic contaminants, are natural sinks and environmental reservoirs for PAHs in the aquatic environment, and they offer an irreplaceable aid in the development of sediment quality criteria (Santana et al., 2015). Therefore, a comprehensive study of PAH behavior in aquatic environments has been of great concern because riverine and estuarine areas receive considerable amounts of pollutant inputs from terrestrial drainage, which could potentially threaten aquatic organism (Tavakoly Sany et al., 2014; Zhang et al., 2015; Dudhagara et al., 2016).

Historic river of Europe and second biggest river in Italy, the Tiber River is the most polluted river among the twenty longest river in Italy (Legambiente, 2006). Especially in the lower course of the river Tiber, after the confluence with its major tributary, the heavy polluted Aniene River, the river water quality decreases dramatically due to discharges from intense industrial activities, heavily urbanized watershed and agricultural waste (Bettinetti et al., 2011). Indeed Tiber River watershed, estuary and the adjacent coastal area is now experiencing serious pollution stress. However, few of the recent studies reported data on the occurrence of PAHs contamination only around the urban areas of Tiber River Basin (Minissi et al., 1998; Patrolecco et al., 2010); and, to the best of our knowledge, no data are available on the occurrence, environmental risk and source of PAHs in the final stretch of Tiber River and its discharge into the estuary and adjacent coastal area. Hence, we aimed to investigate the levels, spatial distribution and sources of PAHs in the Tiber River and its Estuary. The ecological risk assessment of PAHs was also conducted to provide scientific data for organic pollution control of the coast.

The present study is part of a large project aimed to contribute to the knowledge of the pollution affecting the Tiber River and its environmental impact on the Mediterranean Sea. The aim of this project is to assess the pollution due to effluents from local industries, agriculture and the urban impact by identifying several groups of organic and inorganic chemicals and some indicators of microbial pollution in water and sediments. This paper reports the data on the contamination caused by PAHs drained into the Tiber River and its environmental impact on the Mediterranean Sea.

2. Material and methods

2.1. Study area and sampling

The Tiber River rises in the Appenine Mountains (Central Italy) and flows through six regions of Central Italy, crosses densely populated urban area of Rome before flowing into the Tyrrhenian Sea (Central Mediterranean Sea). With a length of 409 km and an annual mean flow rate of 230 $m^3\ s^{-1}$, the Tiber River is an important water resource for industrial production, agricultural irrigation and community livelihood (Patrolecco et al., 2015). Moreover, the Tiber River receives significant urban discharges from Rome, the largest agricultural district in Europe and the most populated city of Italy, with a population of about 2,863,322 residents and an average density of 2224/km^2 (ISTAT, 2010, 2014). Two major wastewater treatment plants, that treat wastewater collected near the Northern and Southern ends of the urban stretch, with an annual average discharges of 3–3.5 $m^3\ s^{-1}$ and 8–9 $m^3\ s^{-1}$, seem to be unable to remove the entire load of pollutants (Patrolecco et al., 2010; di Lascio et al., 2013). As a consequence, this River receives huge amount of incompletely treated domestic sewage and pollutants produced by industry and agriculture, that leads to ecological dangerous consequences.

In this study, four sampling campaigns were conducted in August 2014, November 2014, February 2015 and May 2015 in order to assess temporal trends of pollutants. In each campaign were sampled 21 location: three locations were sampled before and after the fork in the river, in order to have a proper idea of the evolution of the contamination downriver (Fig. 1). In addition, nine points were sampled in the continental shelf around the Tiber artificial mouth (Fiumicino canal) and other nine points in the continental shelf around the Tiber natural mouth (Fiumara Grande) to assess the environmental impact of the Tiber River on the Mediterranean Sea. Three points were sampled 500 m from the Tiber River mouths, another three points 1000 m away and, finally, another three points 1500 m from the river mouths (Fig. 1). The coordinates of sampling sites are given in Table 1.

In each sampling point 2.5 L of water (one amber bottles) were collected and transported refrigerated (4 °C) to the laboratory. Surface sediment (0–5 cm) samples were collected by using a grab sampler (Van Veen Bodemhappe 2 L capacity) and put in aluminum containers. The sediments were transported refrigerated to the laboratory and kept at −20 °C before analysis.

2.2. PAHs extraction and analyses

The method used for extraction and cleanup has been published previously (Montuori and Triassi, 2012). Briefly, water samples were filtered through a previously kiln-fired (400 °C overnight) GF/F glass fiber filter (47 mm × 0.7 μm; Whatman, Maidstone, UK). Filters (suspended particulate matter, SPM) were kept in the dark at −20 °C until analysis. Dissolved phases (fraction of contaminants passing through the filter) were kept in the dark at 4 °C and extracted within the same day of sampling (3–6 h from sampling).

Filters were spiked with three-surrogate standards (10 ng of chrysene-$_{d12}$, benzo[*a*]pyrene-$_{d12}$ and indeno[1,2,3-*cd*]pyrene-$_{d12}$) and extracted three times by sonication with 10 mL of dichloromethane-methanol (1:1) (Carlo Erba, Milano, Italy) for 15 min. After extraction, the extracts were concentrated using a rotary evaporator. The volume of the extracts was adjusted to 0.5 mL and solvent-exchanged into hexane (Carlo Erba). Clean up and fraction procedures were performed with open column chromatography (3 g of neutral alumina Carlo Erba, deactivated with 3% (w/w) Milli-Q water. Three fractions were collected: fraction I with 5.5 mL of hexane (Carlo Erba), fraction II with 6 mL of hexane:ethylacetate (9:1) (Carlo Erba) and, finally, fraction III with 12 mL of ethylacetate (fraction III or F3).

The dissolved phase was spiked with a surrogate solution of chrysene-$_{d12}$, benzo[*a*]pyrene-$_{d12}$ and indeno[1,2,3-*cd*]pyrene-$_{d12}$ in methanol achieving a final concentration in water of 10 ng L^{-1}. Two liter of previously filtered water (DP, dissolved phase) were preconcentrated by solid phase extraction (SPE) using a 100 mg polymeric phase cartridge Strata X™ from Phenomenex (Torrance, CA, USA). After eluting with 10 mL ethylacetate-hexane (1:1), the extract was rotaevaporated to roughly 0.5 mL. The sample was fractionated using an alumina open column chromatography as indicated above for the particulate phase.

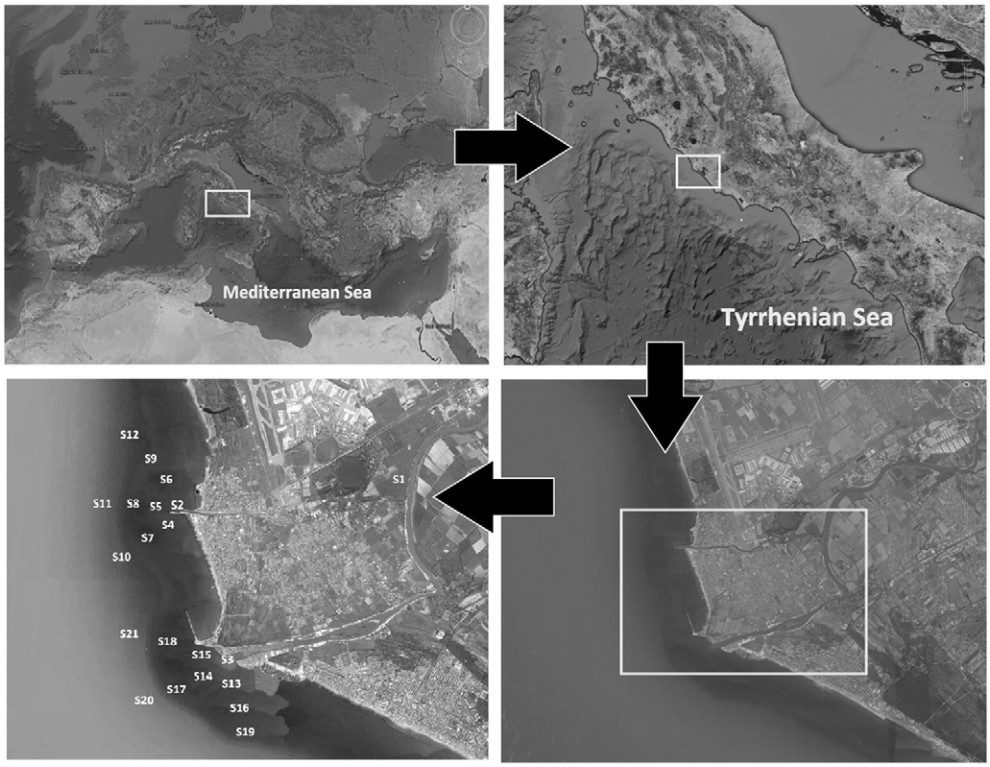

Fig. 1. Map of the study areas and sampling sites in the Tiber River and Estuary, Central Italy. (From Google Earth).

Sediments were oven dried at 60 °C and sieved at 250 μm. Then, 5 g of sediment were spiked with the surrogate mixture (10 ng of chrysene-$_{d12}$, benzo[*a*]pyrene-$_{d12}$ and indeno[1,2,3-*cd*]pyrene-$_{d12}$) and extracted three times by sonication using 15 mL of DCM/methanol (1:1) for 15 min. After centrifuging, the organic extract were concentrated and fractionated in the same way than the water samples. In addition, total organic carbon (TOC) in the sediment samples was determined by TOC analyzer (TOC-VCPH, Shimadzu Corp., Japan).

Cleaned extracts of fractions II were analyzed by GC–MS QP2010 Plus Shimadzu (Kyoto, Japan), equipped with a AOC-20i Shimadzu (Kyoto, Japan) autosampler, operating in the electron impact mode at 70 eV. A Rxi 5Sil MS capillary column (5% phenyl 95% dimethylpolysiloxane) (30 m, 0.25 mm ID and 0.10 μm of film thickness) was used. The column temperature was programmed as follows: first, heated to 60 °C and held for 2 min; ramped to 200 at 25 °C min^{-1}; then ramped to 270 at 10 °C min^{-1} and held for 6 min; and finally ramped to 310 at 25 °C min^{-1} and held for 10 min. Helium was used as carrier gas. The injection port temperature was 300 °C and it was operated in pulsed splitless mode. Acquisition was carried out in the single ion monitoring mode (SIM) using two characteristic ions for each target analyte. Target analytes were identified and verified by comparing retention times of the samples with standards and using the characteristic ions and their ratio for each target analyte. Furthermore, for the higher concentrated samples, the identification of target analytes was confirmed in full-scan mode (*m/z* range from 60 to 350) and were quantified using the internal using the characteristic ions and their ratio for each target analyte.

The concentration was calculated from the calibration curves for the 16 PAHs (Dr. Ehrenstorfer GmbH, Augsburg, Germany) ($r^2 > 0.98$). Triphenylamine was used as internal standard to compensate for the sensitivity variation of the MS detector. In each sample the concentration of following sixteen selected PAHs monitored by the US Environmental Protection Agency (USEPA) as priority pollutants were measured: naphthalene (Nap), acenaphthylene (Acy), acenaphthene (Ace), fluorene (Flu), phenanthrene (Phe), anthracene (An), fluoranthene (Fl), pyrene (Pyr), benzo[*a*]anthracene (BaA), chrysene (Chr), benzo[*b*]fluoranthene (BbF), benzo[*k*]fluoranthene (BkF), benzo[*a*]pyrene (BaP), dibenzo[*a,h*]anthracene (DahA), benzo[*ghi*]perylene (BghiP) and indeno[1,2,3-*cd*]pyrene (InP). Moreover, perylene (Per), not included in this list, also were monitored. Total PAHs concentration were calculated as the sum of the concentrations of the 16 PAHs compounds (ΣPAHs) selected by the USEPA as priority pollutants.

2.3. Quality assurance and quality control

The limit of detection (LOD) and limit of quantification (LOQ) were calculated as having signal-to-noise ratios of above 3 and 10, respectively, by five replicate analyses. The mean surrogate recoveries in the dissolved phase were 89.3 ± 5.7% for chrysene-$_{d12}$, 95.2 ± 7.5% for benzo[*a*]pyrene-$_{d12}$ and 96.8 ± 8.2% for indeno[1,2,3-*cd*]pyrene-$_{d12}$. In the SPM samples, recoveries were 91.2 ± 5.9% for chrysene-$_{d12}$, 96.3 ± 5.5% for benzo[*a*]pyrene-$_{d12}$ and 97.7 ± 9.5% for indeno[1,2,3-*cd*]pyrene-$_{d12}$. Finally, in the sediment samples the averaged recoveries were the following: 87.8 ± 10.3% for chrysene-$_{d12}$, 92.2 ± 9.7% for benzo[*a*]pyrene-$_{d12}$ and 99.5 ± 12.3% for indeno[1,2,3-*cd*]pyrene-$_{d12}$. Procedural blanks were routinely analyzed after every 5 samples; no interferences were detected in the blanks. Blank assays were carried out and used for the calculation of LODs and LOQs. In the dissolved phase, LODs ranged from 0.01 ng L^{-1} for pyrene to 0.1 ng L^{-1} for indeno[1,2,3-*cd*]pyrene while, in SPM and sediment samples, from 0.03 to 0.2 ng L^{-1} and from 0.01 to 0.15 ng g^{-1} respectively. The quantification limits (LOQ) was in the range of 0.02 ng L^{-1} – 0.15 ng L^{-1} in dissolved water samples, 0.06–0.3 ng L^{-1} in SPM samples and 0.03 to 0.2 ng g^{-1} in sediment samples. Reported concentrations were corrected by surrogates recoveries.

2.4. Statistical analysis and calculation of PAHs inputs

Statistical analysis of the results was carried out with the statistical software SPSS, version 14.01 for Windows (SPSS Inc., Chicago, IL,

Table 1
Description of the sampling sites and concentrations of PAHs in the water dissolved phase (DP), suspended particulate matter (SPM) and sediments of the Tiber River and the continental shelf, Central Italy.

Sampling location			∑PAHs								
Site number identification	Site characteristics	Site location	DP (ng L^{-1})				SPM (ng L^{-1}) (ng g^{-1} dry wt.)				Sediment (ng g^{-1} dry wt.)
			Aug 2014	Nov 2014	Feb 2015	May 2015	Aug 2014	Nov 2014	Feb 2015	May 2015	May 2015
1 (river water)	Upstream Tiber River fork	41°46′40.65″N 12°16′45.62″E	607.5	376.3	122.2	492.2	344.2 (842.1)	323.6 (3667.2)	473.4 (1232.5)	318.2 (627.2)	545.6
2 (river water)	Tiber River Mouth Fiumicino Canal	41°46′17.34″N 12°13′06.37″E	321.3	233.8	42.7	387.6	232.9 (593.1)	233.3 (2297.2)	396.9 (724.1)	261.7 (577.8)	398.9
3 (river water)	Tiber River MouthFiumara Grande	41°44′24.50″N 12°13′58.73″E	270.8	112.5	66.5	304.6	140.8 (471.1)	104.8 (1392.0)	252.9 (1499.4)	123.9 (428.0)	287.1
4 (sea water)	River Mouth Fiumicino Canal at 500 m South	41°46′01.74″N 12°12′56.67″E	105.3	53.2	29.2	92.6	153.2 (730.3)	149.7 (2776.1)	202.1 (2160.0)	172.1 (1007.4)	175.9
5 (sea water)	River Mouth Fiumicino Canal at 500 m Central	41°46′17.84″N 12°12′44.76″E	117.4	56.1	25.6	88.8	84.5 (427.6)	101.2 (2061.7)	137.9 (3605.0)	96.1 (1195.4)	107.3
6 (sea water)	River Mouth Fiumicino Canal at 500 m North	41°46′31.73″N 12°12′53.50″E	456.1	237.5	146.1	365.6	273.1 (3117.0)	212.3 (2746.9)	348.1 (5166.9)	240.9 (665.8)	297.6
7 (sea water)	River Mouth Fiumicino Canal at 1000 m South	41°45′47.87″N 12°12′53.50″E	78.2	27.6	11.6	55.7	105.7 (1143.1)	101.3 (1665.1)	133.0 (4857.5)	121.9 (2775.8)	86.5
8 (sea water)	River Mouth Fiumicino Canal at 1000 m Central	41°46′17.30″N 12°12′20.34″E	30.5	12.2	22.8	24.0	76.1 (3490.6)	54.0 (585.2)	65.8 (1800.5)	58.5 (545.8)	64.3
9 (sea water)	River Mouth Fiumicino Canal at 1000 m North	41°46′46.51″N 12°12′41.74″E	162.3	77.0	88.1	122.7	206.2 (592.6)	144.9 (3426.6)	207.1 (2853.7)	162.3 (725.8)	170.0
10 (sea water)	River Mouth Fiumicino Canal at 1500 m South	41°45′33.77″N 12°12′40.43″E	15.6	7.86	11.2	18.3	64.8 (918.5)	50.2 (1742.4)	50.9 (2585.1)	49.7 (619.1)	61.0
11 (sea water)	River Mouth Fiumicino Canal at 1500 m Central	41°46′16.33″N 12°12′01.41″E	13.8	5.59	7.78	7.73	31.0 (333.4)	19.6 (581.1)	25.4 (307.2)	22.6 (30.5)	47.7
12 (sea water)	River Mouth Fiumicino Canal at 1500 m North	41°46′58.36″N 12°12′29.55″E	43.1	19.7	14.8	35.3	90.3 (670.4)	71.3 (1038.7)	95.5 (2729.6)	103.9 (1007.9)	84.0
13 (sea water)	River Mouth Fiumara Grande at 500 m South	41°44′08.68″N 12°14′07.38″E	258.8	150.2	81.3	190.6	145.2 (2601.7)	127.7 (1032.5)	214.7 (4576.2)	112.2 (332.4)	267.9
14 (sea water)	River Mouth Fiumara Grande at 500 m Central	41°44′14.43″N 12°13′40.05″E	51.7	22.8	29.7	47.2	71.3 (425.6)	43.3 (490.2)	64.4 (224.3)	40.9 (186.7)	63.7
15 (sea water)	River Mouth Fiumara Grande at 500 m North	41°44′27.27″N 12°13′36.50″E	116.2	82.5	9.38	99.8	53.8 (264.3)	54.5 (758.3)	119.9 (1811.3)	54.8 (622.3)	170.1
16 (sea waer)	River Mouth Fiumara Grande at 1000 m South	41°43′52.67″N 12°14′13.37″E	64.5	43.7	38.8	55.7	78.0 (201.4)	65.9 (952.3)	99.8 (1790.3)	47.9 (287.7)	125.4
17 (sea water)	River Mouth Fiumara Grande at 1000 m Central	41°44′06.84″N 12°13′20.15″E	12.7	4.78	7.92	10.9	27.4 (300.8)	29.9 (508.0)	28.4 (1103.6)	22.4 (32.8)	42.9
18 (sea water)	River Mouth Fiumara Grande at 1000 m North	41°44′28.80″N 12°13′12.00″E	33.9	26.6	10.4	36.5	30.8 (502.4)	25.8 (565.3)	68.5 (1589.7)	29.2 (1305.0)	90.4
19 (sea water)	River Mouth Fiumara Grande at 1500 m South	41°43′38.09″N 12°14′18.04″E	21.9	7.19	8.63	16.6	32.1 (739.9)	26.1 (1154.5)	48.4 (621.2)	19.8 (372.1)	90.9
20 (sea water)	River Mouth Fiumara Grande at 1500 m Central	41°43′59.84″N 12°13′01.01″E	4.22	1.75	2.83	2.88	15.9 (192.1)	11.2 (133.8)	15.3 (614.2)	9.82 (375.5)	36.2
21 (sea water)	River Mouth Fiumara Grande at 1500 m North	41°44′32.41″N 12°12′52.76″E	9.75	2.28	2.60	6.00	14.0 (141.4)	8.00 (215.8)	15.5 (373.9)	4.53 (123.4)	46.8

USA). All data was presented as the mean ± standard deviation (SD). The level of significance was set at $p < 0.05$.

The method used to estimate the annual contaminant discharges (F_{annual}) was based on the UNEP guidelines (UNEP/MAP, 2004), and has been widely accepted (Walling and Webb, 1985; HELCOM, 1993; Steen et al., 2001; Montuori and Triassi, 2012). A flow-averaged mean concentration (C_{aw}) was calculated for the available data, which was corrected by the total water discharge in the sampled period. The equations used were the following:

$$C_{aw} = \frac{\sum^{n}_{i=1} C_i Q_i}{\sum^{n}_{i=1} Q_i} \quad (1)$$

$$F_{annual} = C_{aw} Q_T \quad (2)$$

where C_i and Q_i are the instantaneous concentration and the daily averaged water flow discharge, respectively for each sampling event (flow discharge, section and bed elevation of river mouth were measured by manual probes). Q_T represents the total river discharge for the period considered (August 2014–May 2015), calculated by adding the monthly averaged water flow. River flow data was collected from the register of the Autorità di Bacino del Tevere to http://www.abtevere.it (Lazio Government for the Environment). Furthermore, to study the temporal contaminant discharge variation, C_i and Q_i were considered for each campaign and expressed as kg $year^{-1}$.

Principal Component Analysis (PCA) was performed using SPAD (Systeme Portable pour l'Analyse des Données) to display the pattern of similarity of the observations (sampling sites) and of the variables as points. In the PCA, when concentrations were below the LOQ, a value of half the LOQ was used.

2.5. Potential toxicity of PAHs

Ecological risk assessment was performed to evaluate the possibility of adverse ecological effect. A widely used assessment method is based on toxic equivalent factors (TEFs) (Nisbet and LaGoy, 1992). The toxicity assessment of sediments from Tiber River and its Estuary was carried out according to the total concentration of some high molecular weight PAHs (BaA, Chr, BbF, BkF, BaP, InP and DahA) that were considered toxic

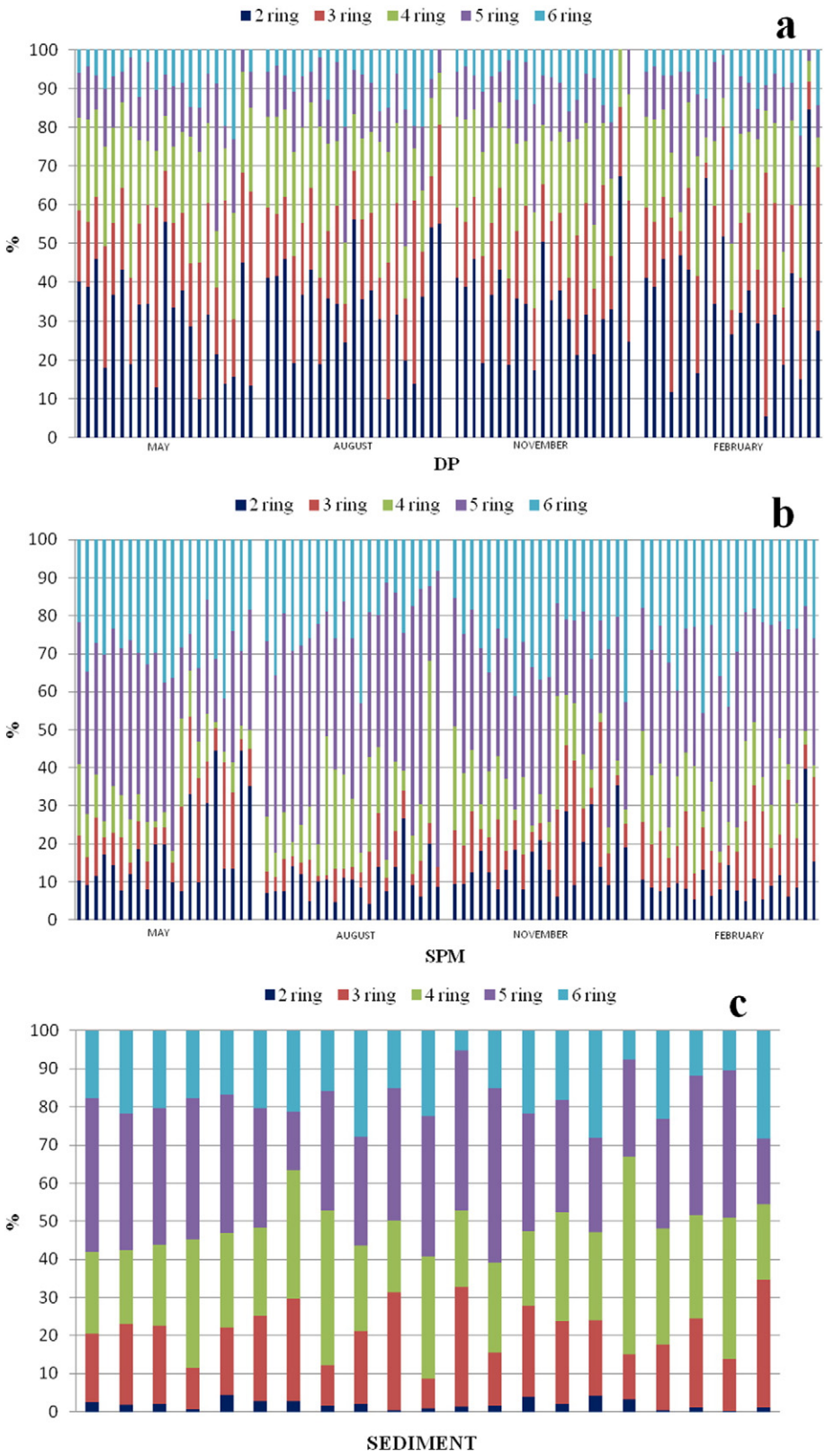

Fig. 2. Composition pattern of total PAHs in water dissolved phase (DP; a), in suspended particulate matter (SPM; b) and in sediments (c) of the Tiber River and the continental shelf, Central Italy.

Table 2
Concentration ranges and mean value of PAHs in water, suspended particulate matter (SPM) and sediments from recent studies of different rivers, estuaries and coasts in the world.

Area	References	Number PAHs	Range ∑PAHs	Mean ∑PAHs
Water (ng L^{-1})				
Xijiang River, China	Deng et al. (2006)	15	21.7–138.0	–
Yellow River, China	Li et al. (2006)	15	179.0–369.0	248.2
Daliao River, China	Guo et al. (2009)	18	570.2–2318.6	–
Henan Reach of Yellow River, China	Sun et al. (2009)	16	144.3–2361.0	662.0
Tiber River, Italy	Patrolecco et al. (2010)	6	23.9–72.0	43.4
Gomti River, india	Malik et al. (2011)	16	60–84,210.0	10,330.0
Gulf of Tunis, Tunisia	Mzoughi and Chouba (2011)	22	139.2–1008.3	–
Songhua River, China	Ma et al. (2013)	15	14.0–161.0	33.9
Mediterranean Sea	Berrojalbiz et al. (2011)	19	0.158–3.656	0.605
Wyre River, England	Moeckel et al. (2013)	28	2.7–20.0	–
Taizi River, China	Song et al. (2013)	15	223.0–5794.0	1818.0
Liaohe River, China	Bai et al. (2014)	16	111.9–2931.6	454.7
Marseilles coastal area, France	Guigue et al. (2014)	32	8.1–405.0	–
Liaohe River, China	Lv et al. (2014)	16	94.8–2931.6	396.5
Danube River, Hungary	Nagy et al. (2014)	16	25.0–1208.0	122.6
Songhua River, China	Zhao et al. (2014)	16	163.5–2746.2	934.6
Tampa Bay, Florida	Lewis and Russell (2015)	16	<lod	–
Almendares River, Cuba	Santana et al. (2015)	14	836.0–15,811.0	2512.0
Elbe and Weser Rivers, Germany	Siemers et al. (2015)	16	10.0–40.0	–
Jiulong River Estuary, China	Wu et al. (2015)	15	28.6–48.5	39.0
Yellow River, China	Zhang et al. (2015)	16	38.3–222.4	94.3
Yellow River, China	Zhao et al. (2015)	16	548.0–2598.0	1375.0
Poyang Lake, China	Zhi et al. (2015)	16	5.6–266.1	–
Cauca River, Colombia	Sarria-Villa et al. (2016)	12	52.1–12,888.2	2344.5
Daliao River estuary, China	Zheng et al. (2016)	16	71.1–4255.4	748.8
SPM (ng L^{-1})				
Xijiang River, China	Deng et al. (2006)	15	1.4–58.1	29.8
Yellow River, China	Li et al. (2006)	13	54.0–155.0[a]	–
Daliao River, China	Guo et al. (2009)	18	151.0–28,483.8	–
Henan Reach of Yellow River, China	Sun et al. (2009)	16	506.6–10,510.0*	4100.0*
Tiber River, Italy	Patrolecco et al. (2010)	6	37.6–47.0	
Mediterranean Sea	Berrojalbiz et al. (2011)	19	0.033–0.380	0.129
Gulf of Tunis, Tunisia	Mzoughi and Chouba (2011)	22	909.9–8222.4*	–
Songhua River, China	Ma et al. (2013)	15	9.21–83.1	26.4
Yellow River, China	Zhao et al. (2015)	16	1502.0–11,562.0*	5591.0*
Daliao River estuary, China	Zheng et al. (2016)	16	1969.9–11,612.2	4015.7
Sediment (ng g^{-1})				
Tiber River, Italy	Minissi et al. (1998)	13	4.5–652.2	–
Yellow River, China	Li et al. (2006)	13	31.0–133.0	76.8
Daliao River, China	Guo et al. (2009)	18	102.9–3419.2	–
Henan Reach of Yellow River, China	Sun et al. (2009)	16	16.4–1358.0	182.0
Cocó and Ceará Rivers, Brazil	Cavalcante et al. (2009)	17	3.0–2234.8	–
Tiber River, Italy	Patrolecco et al. (2010)	6	157.8–271.6	215.2
Gomti River, india	Malik et al. (2011)	16	5.24–3722.87	697.2
Gulf of Tunis, Tunisia	Mzoughi and Chouba (2011)	22	363.3–7026.4	–
Italian Marine Protected Areas, Italy	Perra et al. (2011)	16	0.7–1550.0	155.3
Ammer River, Germany	Liu et al. (2013)	16	112.0–22,900.0	8770.0
Songhua River, China	Ma et al. (2013)	15	20.5–632.0	178.0
Marano and Grado Lagoon. Italy	Acquavita et al. (2014)	16	50.0–1026.0	–
Liaohe River, China	Bai et al. (2014)	16	92.2–295,635.2	8432.6
Gulf of Trieste, Italy	Bajt (2014)	16	214.0–4416.0	–
Shenzhen River, China	Deng et al. (2014)	16	828.0–1320.0	1028
Priolo Bay, Italy	Di Leonardo et al. (2014)	18	56.4–847.1	–
Huveaune River, France	Kanzari et al. (2014)	16	571.7–4234.9	1966.00
Iberian coast, Spain	León et al. (2014)	13	5.3–2627.4	–
Ibirité Reservoir, Brazil	Mozeto et al. (2014)	16	79.8–219.9	129.5
Danube River, Hungary	Nagy et al. (2014)	16	8.3–1202.5	170.0
Songhua River, China	Zhao et al. (2014)	16	68.2–654.1	234.1
Caspian sea coast, India	Yancheshmeh et al. (2014)	23	1294.0–9009.0	3228.0
Portimão Harbor, Portugal	Bebianno et al. (2015)	16	218.0–1690.0	–
Baffin Bay, Canada	Foster et al. (2015)	66	341.0–2693.0	–
Durance River, France	Kanzari et al. (2015)	16	57.0–1528.0	–
Tampa Bay, Florida	Lewis and Russell (2015)	16	1.7–147.9	18.0
Yellow Sea, China	Li et al. (2015a)	16	148.3–907.5	548.6
Bohai Sea, China			149.2–1211.8	481.2
Beibu Gulf, China	Li et al. (2015b)	15	3.3–388.0	47.8
Hun River, China	Liu et al. (2015)	15	82.9–39,292.9	3705.5
Bahia Blanca Estuary, Argentina	Oliva et al. (2015)	17	19.7–30,054.5	1798.5
Ría de Arousa, Spain	Pérez-Fernández et al. (2015)	35	45.0–7901.0	–
Mithi River, India	Singare (2015)	17	1206.0–4735.0	2824.0
Ölüdeniz Lagoon, Turkey	Tuncel and Topal (2015)	16	–	1850.0
Bohai Bay, China	Wang et al. (2015a)	16	24.6–280.6	79.3
Erjien River, Taiwan	Wang et al. (2015b)	16	22.0–28,622.0	737.0

(continued on next page)

Table 2 (*continued*)

Area	References	Number PAHs	Range ∑PAHs	Mean ∑PAHs
Yangtze River, China	Yu et al. (2015)	16	65.1–954.5	229.9
Yellow River, China	Zhao et al. (2015)	16	181.0–1583.0	810.0
Hangzhou Bay, China	Adeleye et al. (2016)	10	32.1–171.1	–
Cauca River, Colombia	Sarria-Villa et al. (2016)	12	ND-3739.0	1028.0
Daliao River estuary, China	Zheng et al. (2016)	16	374.8–11,588.8	3700.3
This study	DP	16	*1.75–607.5*	*90.5 ± 125.1*
	SPM		*4.53–473.4*	*111.5 ± 100.1*
	Sediment		*36.2–545.6*	*155.3 ± 134.1*

ND: not detectable.
* ng g.

PAHs due to their mutagenic and carcinogenic effect on human and other organism (Nisbet and LaGoy, 1992; Tavakoly Sany et al., 2014). Among the seven carcinogenic PAHs, BaP is the only one having sufficiently toxicological data for derivation of a carcinogenic factor (Pérez-Fernández et al., 2015; Sarria-Villa et al., 2016). According to the USEPA (2012), TEFs for BaA, Chr, BbF, BkF, BaP, InP, and DahA were 0.1, 0.001, 0.1, 0.01, 1, 0.1 and 1, respectively. The total toxic equivalent quantity (TEQ_{PAHs}) in each site was calculated using the following equation:

$$TEQ_{PAHs} = \Sigma TEFi \text{ x } CcPAHi \quad (3)$$

where CcPAHi is the carcinogenic PAH concentration (ng g^{-h} dw); TEFi is the toxic factor of each cPAH relative to benzo[*a*]pyrene.

3. Results and discussions

3.1. PAHs concentrations in water dissolved phase

The concentrations of total PAHs detected in the water dissolved phase (DP) collected at 21 sites from Tiber River and its Estuary ranged from 1.75 (site 20) to 607.5 (site 1) ng L^{-1} with a mean value of 90.5 ± 125.1 ng L^{-1} (Table 1). In detail, they ranged from 0.53 to 249.2 ng L^{-1} with a mean value of 33.7 ± 52.8 ng L^{-1} for 2-ring PAHs (Nap), from 0.21 to 110.4 ng L^{-1} for 3-ring PAHs (Acy, Ace, Flu, Phe, An), from 0.15 to 142.6 ng L^{-1} for 4-ring PAHs (Fl, Pyr, BaA, Chr), from 0.08 to 70.2 ng L^{-1} for 5-ring PAHs (BbF, BkF, BaP, DahA) and from 0.15 to 35.1 ng L^{-1} for 6-ring PAHs (BghiP, InP). The compositional profiles of PAH in the dissolved phase are illustrated in Fig. 2a, which indicates that 2- and 3-ring PAHs were abundant in all sampling sites, representing on average over 58% of all PAHs. In addition, the 5– and 6-ring PAHs were present in low concentrations, accounting for only 19% of total PAHs. The prevalence of low molecular weight PAHs (2–3-ring) in the water could be explained by their high water solubility and relatively high vapor pressures (Santana et al., 2015; Zhao et al., 2015; Sarria-Villa et al., 2016).

Compared with other polluted rivers in the world (Table 2), the concentrations of ΣPAHs in the dissolved phase from the Tiber River (1.75–607.5 ng L^{-1}) were much higher than those found in the Wyre River (England) by Moeckel et al. (2013), in the Jiulong River (China) by Wu et al. (2015) and in the Elbe and Weser Rivers (Germany) by Siemers et al. (2015); these levels were however lower than those found in China in the Songhua River (Ma et al., 2013) and in the Cauca River (Sarria-Villa et al., 2016). Based on these results, the levels of PAHs in the dissolved phase in the Tiber River are comparable to those found in China in the Yellow River, by Li et al. (2006) and in the Marseilles Coastal area by Guigue et al. (2014). In comparison to open Mediterranean sea (Berrojalbiz et al., 2011), the total PAHs concentrations in the dissolved phase of the Tiber River Estuary were much higher probably due to maritime transport, coastal anthropogenic activities and municipal treatment discharges (Table 2).

3.2. PAHs concentrations in suspended particulate matter

The concentrations of PAHs in the suspended particulate matter (SPM) samples range from 4.53 ng L^{-1} (123.4 ng g^{-1} dry weight) in site 21 to 473.4 ng L^{-1} (1232.5 ng g^{-1} dry weight) in site 1 (mean value of 111.5 ± 100.1 ng L^{-1}), as shown in Table 1. The concentrations of PAHs detected ranged from 1.23 to 49.7 ng L^{-1} with a mean value of 11.3 ± 8.71 ng L^{-1} for 2-ring PAHs (Nap), from 3.47 to 72.7 ng L^{-1} for 3-ring PAHs (Acy, Ace, Flu, Phe, An), from 0.48 to 112.3 ng L^{-1} for 4-ring PAHs (Fl, Pyr, BaA, Chr), from 5.20 to 158.5 ng L^{-1} for 5-ring PAHs (BbF, BkF, BaP, DahA) and from 4.03 to 115.0 ng L^{-1} for 6-ring PAHs (BghiP, InP). The compositional profiles of PAHs in SPMs are illustrated in Fig. 2b; this figure shows that 4-, 5-, 6-ring PAHs were abundant at most sampling sites, accounting for 15%, 38%, and 26% of ΣPAHs in SPMs, respectively.

The proportion of high molecular weight PAHs increased to 79%, much above than in dissolved samples, where it was 42%. The results indicated that high molecular weight PAHs were preferentially absorbed by the particulate matter due to their high hydrophobicity and hardly biodegraded, volatilized properties and larger octanol–water partition coefficients (Kow), in agreement with the PAHs partition theory (Patrolecco et al., 2010; Mzoughi and Chouba, 2011; Zhao et al., 2015). Indeed, the partition coefficients (Kp, defined as the ratio of the concentration of a chemical associated with SPM to that in the DP: $Kp = C_{SPM}/C_{DP}$) showed an increasing trend of high-ring compounds in their SPM partitioning (average value of 1.77, 8.53 and 11.2 respectively for 4-, 5-, 6-ring PAHs).

Compared with other polluted rivers in the world (Table 2), PAHs in SPMs from the Tiber River were close to those found in the Yellow River, China (Li et al., 2006). The concentrations were much higher than those presented in the Songhua River, China (Ma et al., 2013) and in the Xijiang River, China (Deng et al., 2006), but lower than those found in China in the Daliao River (Guo et al., 2009; Zheng et al., 2016), and in the Gulf of Tunis, Tunisia (Mzoughi and Chouba, 2011).

3.3. PAHs concentrations in sediments

The concentrations of total PAHs in sediment samples are illustrated in Table 1. Results range from 36.2 (site 20) to 545.6 (site 1) ng g^{-1} with a mean value of 155.3 ± 134.1 ng g^{-1}. The concentrations detected ranged from 0.06 to 13.4 ng g^{-1} with a mean value of 3.29 ± 3.39 ng g^{-1} for 2-ring PAHs (Nap), from 3.69 to 98.8 ng g^{-1} for 3-ring PAHs (Acy, Ace, Flu, Phe, An), from 9.35 to 117.1 ng g^{-1} for 4-ring PAHs (Fl, Pyr, BaA, Chr), from 7.98 to 219.1 ng g^{-1} for 5-ring PAHs (BbF, BkF, BaP, DahA) and from 3.25 to 97.2 ng g^{-1} for 6-ring PAHs (BghiP, InP). As concerns the compositional profiles of PAH in sediments at each sampling sites, 4- and 5-ring PAHs were abundant at most sites, accounting for 24% and 35% of ΣPAHs in sediments, respectively (Fig. 2c). The difference between PAH pattern in water and sediments may be due to molecular weight and bacterial degradation. High molecular weight PAHs were more resistant to degradation and could been

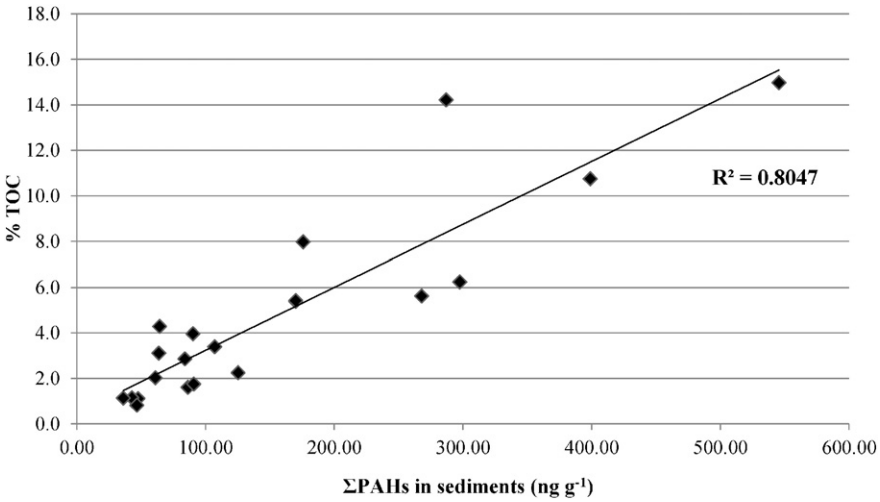

Fig. 3. Relationship between TOC (%) and ΣPAHs in the sediment samples of the of the Tiber River.

efficiently transport to and easily accumulate in the sediments largely unaltered (Liu et al., 2015; Singare, 2015; Zhao et al., 2015). Contrariwise, low molecular weight PAHs were mostly in the dissolved aquatic phase due to their high water solubility and due to benthic recycling, that prevented their incorporation into the bottom sediments. (Baker et al., 1991; Lipiatou et al., 1997; Sun et al., 2009). Indeed, low molecular weight PAHs (such as Nap) are more likely to undergo microbial degradation than higher molecular weight compounds, probably because tendency to biodegradation decreases as the number of fused rings in the PAH increases (Lima et al., 2005).

Compared with other polluted rivers in the world (Table 2), the concentrations of ΣPAHs in the sediment samples from the Tiber River and Estuary (36.2–545.6 ng g^{-1}) were similar to those found in the Priolo Bay (Italy) by Di Leonardo et al. (2014), in the Songhua River, China

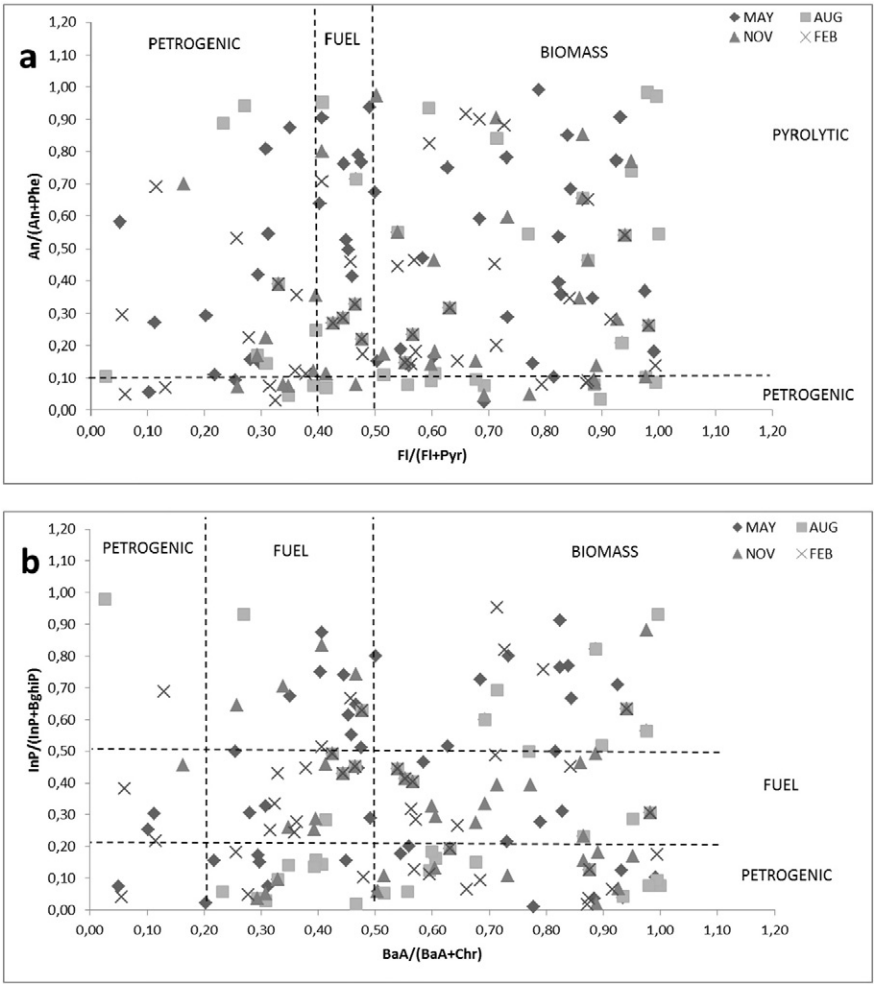

Fig. 4. Cross plots of the values of Fl/(Fl + Pyr) versus An/(An + Phe) (a) and BaA/(BaA + Chr) versus InP/(InP + BghiP) (b) for all samples data of the Tiber River and its estuary.

(Ma et al., 2013; Zhao et al., 2014), in the Yangtze River (China) by Yu et al. (2015) and in the Beibu Gulf (China) by Li et al. (2015b). The concentrations of ΣPAHs in sediment samples from the Tiber River and Estuary were higher than those found in the Ibirité Reservoir, Brazil (Mozeto et al., 2014), in the Bohai Bay, China (Wang et al., 2015a), in the Beibu Gulf, China (Li et al., 2015b) and in the Tampa Bay (Florida) by Lewis and Russell (2015). The concentrations of ΣPAHs in sediment samples from the Tiber River and Estuary were lower than those found in the Huaveaune River (France) by Kanzari et al. (2014), in the Hun River, China (Liu et al., 2015), in the Erjien River, Taiwan (Wang et al., 2015b) and in the Baffin Bay (Canada) by Foster et al. (2015). The concentrations of ΣPAHs in sediments were relatively lower than those present in other rivers and coasts. The low concentrations of PAHs in sediments may be due to the high content of sand and low TOC contents (0.55–10.1 mg g^{-1}, mean 3.20). Fig. 3 showed the relationship between %TOC with the ΣPAHs in the sediment samples. As results showed, a positive linear regression exists between total PAH concentration and TOC data in sediments ($r = 0.80$, $p < 0.01$) as indicated by many other studies (Guo et al., 2009; Sun et al., 2009; Montuori and Triassi, 2012; Sarria-Villa et al., 2016).

3.4. PAHs seasonal and spatial distribution in DP, SPM and sediment samples

The concentrations of total PAHs in DP, SPM and sediment samples of the Tiber River at different sampling sites are illustrated in Table 1 and Fig. S1 (Supplementary material). The results showed that the ratio of the concentration of ΣPAHs in DP samples to that in SPM was less than one in all sites (average 0.71; SD ± 0.56), suggesting that the total amount of PAHs in SPM samples was more abundant than in DP

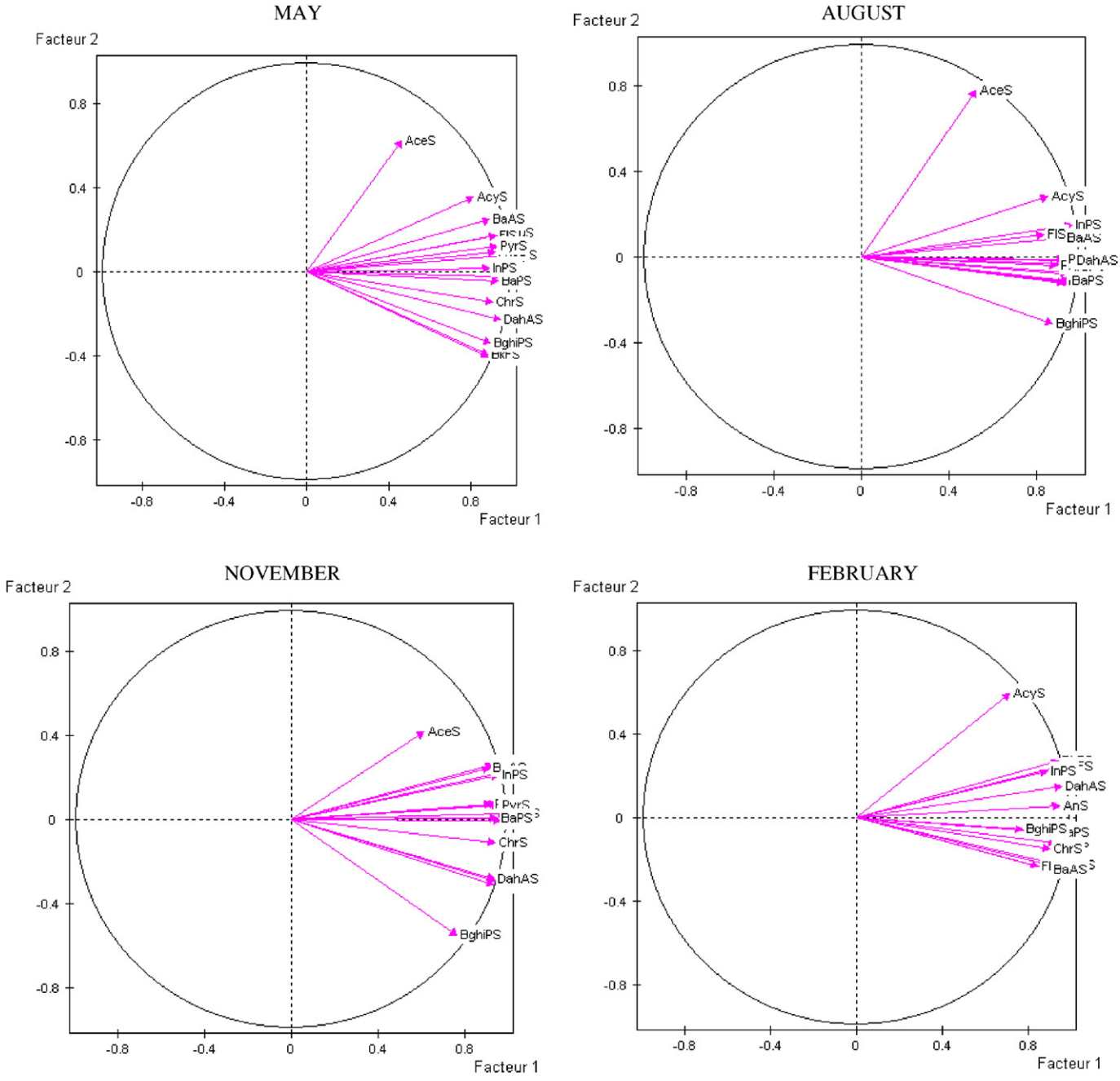

Fig. 5. PCA analysis of PAHs composition of water (sum of DP and SPM) from Tiber River and its Estuary. Loading plot for the first and second PC.

Table 3
A comparison of the TEL, PEL, ERL and ERM guideline values (μg Kg^{-1}) for polycyclic aromatic hydrocarbons and data found in the Tiber River and the continental shelf, Central Italy.

	PAHs																
	Nap	Acy	Ace	Flu	Phe	An	Fl	Pyr	BaA	Chr	BbF	BkF	BaP	DahA	BghiP	InP	∑PAHs
TEL[a]	34.6	5.87	6.71	21.2	86.7	46.9	113	153	74.8	108	–	–	88.8	6.22	–	–	1684
Samples percentage over the TEL	0	29	24	5	0	0	0	0	0	0			0	86			0
PEL[a]	391	128	88.9	144	544	245	1494	1398	693	846	–	–	763	135	–	–	16,770
Samples percentage over the PEL	0	0	0	0	0	0	0	0	0	0			0	0			0
ERL[b]	160	44	16	19	240	85	600	665	261	384	–	–	430	63.4	–	–	4022
Samples percentage over the ERL	0	0	0	5	0	0	0	0	0	0			0	10			0
ERM[b]	2100	640	500	540	1500	1100	5100	2600	1600	2800	–	–	1600	260	–	–	44,792
Samples percentage over the ERM	0	0	0	0	0	0	0	0	0	0			0	0			0

[a] MacDonald et al. (1996).
[b] Long et al. (1995).

samples. Even the total amount of PAHs in SPM samples was more abundant than in sediment samples for each sampling site. Indeed, the ratio of the concentration of ΣPAHs in sediment samples (ng g^{-1}) to that in the SPM samples (expressed in ng g^{-1}) was less than 1 in all sampling sites (average 0.43; range 0.03–1.55; SD ± 0.42). In particular, the PAHs concentrations in DP were significantly lower during the wet season (February) and higher during the dry season (August). This reduction was depending to the hydrological conditions, which caused dilution ratio variations. Therefore, a high river flow rate resulted in a higher dilution ratio in the wet season caused a decrease in the PAHs concentration in both the Tiber River and its estuary. In August, the concentrations of total PAHs in SPM samples were lowest in all sampling sites. These results could be due to the flow decrease during the dry season and consequently huge stagnation of SPM that determined the transfer of the more polar PAHs from SPM to DP. Based on these results, it can be concluded that PAHs loads among the different phases in each sampling site were closely related to the flow variation. Therefore, relatively high concentration of PAHs in SPMs but moderate in sediment indicated that the contamination of PAHs in Tiber River and Estuary might be caused by fresh input of PAHs.

In order to evaluate the huge input of PAHs drained from storm water runoff, tributary inflow, wastewater treatment plant and industrial effluent discharge, agricultural runoff, atmospheric deposition, dredged material disposal, the total load of PAHs into the Tyrrhenian Sea was calculated. The total PAHs loads contribution to the Tyrrhenian Sea from the Tiber River is calculated in about 3161.7 kg $year^{-1}$. Comparing our results with previous published data on Tiber River crossing metropolitan area of Rome (Patrolecco et al., 2010), the PAHs pollution levels in the Tiber River Estuary and its adjacent coastal area increased significantly in the three compartment. As reported by Patrolecco et al. (2010), the PAHs concentrations in urban stretch of the Tiber River ranged from 23.9 to 72.0 ng L^{-1} in surface water, from 37.6 to 353.3 ng L^{-1} in SPM, and from 157.8 to 271.6 ng g^{-1} dw in sediments (Table 2). These results suggested that the PAHs pollution in Tiber River and its Estuary has been aggravating trend since 2007.

The spatial distribution of PAHs in DP, SPM and sediment samples from the Tiber River and its estuary were studied by comparing the concentrations of ΣPAHs in different sampling sites in different seasons. As showed in Fig. S1 (Supplementary material), the PAHs level in the water decreased significantly from site 1 to 2 and 3. Indeed, the total PAHs concentrations decreased to 764.4 ng L^{-1} (DP + SPM mean values of four seasons) at site 1 (Upstream Tiber River fork) to 527.6 ng L^{-1} (DP + SPM mean values of four seasons) at site 2 (Tiber River Mouth Fiumicino canal) and to 344.2 ng L^{-1} (DP + SPM mean values of four seasons) at site 3 (Tiber River Mouth Fiumara Grande). This decrease in total PAHs concentrations is due to the splitting of the river in its two mouths, before flowing into the Tyrrhenian Sea. Moreover, the PAH pollution levels in the estuary and the adjacent area gradually decreased from the vicinity of the river outflows to offshore areas (Fig. S1 in the Supplementary material). At 500 m of river outflow, the concentration of PAHs were similar to those found at Tiber mouths, suggesting that PAHs could be spread by hydrodynamic conditions and frequent water exchange towards the shore. At same time, the PAHs concentrations decreased at 1000 m and even more at 1500 m of the river outflows. Particularly, at the Fiumicino mouth the PAHs loads move into the Tyrrhenian sea northward (Fig. S1a in the Supplementary material). On the contrary, at the Fiumara Grande mouth the PAHs loads move into the Tyrrhenian sea southward (Fig. S1b in the Supplementary material).

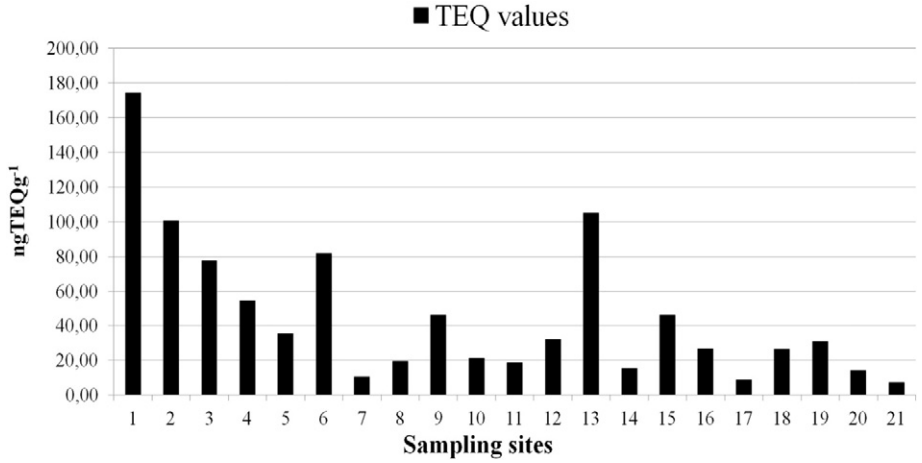

Fig. 6. Total TEQ values in different sites of Tiber River and its Estuary.

3.5. Source identification

PAHs sources can be divided into three classes according to their characteristic fingerprints (Pérez-Fernández et al., 2015; Singare, 2015; Sarria-Villa et al., 2016). The first group is from pyrolytic sources, which includes combustion of fossil fuels, vehicles using gasoline or diesel fuel, waste incineration and coke production, carbon black, coal tar pitch, asphalt and petroleum cracking. The second group is from petrogenic sources, which include crude oil and petrochemicals (gasoline, diesel fuel, kerosene and lubricating oil). Finally, PAHs can also originate from natural processes such as short-term diagenetic degradation of biogenic precursors (diagenesis). Each source (i.e. pyrolytic, petrogenic and diagenetic) gives rise to typical PAH patterns. In general, combustion products are dominated by relatively high molecular weight (HMW) compounds with four or more condensed aromatic rings, whereas bi- and tricyclic aromatic compounds (LMW) are more abundant in fossil fuels, which are, moreover, dominated by alkylated derivatives (Liu et al., 2013; Oliva et al., 2015; Wu et al., 2015). Using chemical profiling and particular compound ratios, it is possible to recognize the processes that generate these compounds (Baumard et al., 1998; Yunker et al., 2002). Among these molecular ratios, An/(An + Phe), Fl/(Fl + Pyr), BaA/(BaA + Chr) and InP/(InP + BghiP) are more widely used (Yunker et al., 2002; Tobiszewski and Namiesnik, 2012). Although the use of PAH diagnostic ratios for source has been criticized (Katsoyiannis et al., 2007; Galarneau, 2008), it has been used widely and consequently, in the present study it is utilized as an indicative tool of PAHs source and distribution.

The ratio study reflected a prevailing pattern of pyrolytic inputs of PAHs in the Tiber River and its estuary. In fact, the results showed that An/(An + Phe) ratio was >0.1 in DP, SPM and sediments (mean 0.38, 0.31 and 0.64, respectively), which attributed the origin of PAHs to pyrogenic sources (Fig. 4a). Also the Phe/An ratio was used to discern the sources of sedimentary PAHs between petrogenic (Phe/An >10) and pyrogenic (Phe/An <10) PAH. Although Phe may be the result of background occurrence such as biogenic sources (Wilcke, 2007; Cabrerizo et al., 2011), the results showed that the Phe/An ratio was <10 at most sites (mean 0.73), suggesting pyrogenic sources such as emissions from combustion of gasoline (Lima et al., 2005). Furthermore, Fl/(Fl + Pyr) ratios differentiate petroleum input from combustion processes (Yunker et al., 2002; Ekpo et al., 2012). For Fl/(Fl + Pyr), low ratios (<0.40) indicate petroleum, intermediate ratios (0.40–0.50) liquid fossil fuel combustion, whereas ratios >0.50 are characteristic of grass, wood, or coal combustion. In the Tiber River and Estuary, ratio Fl/(Fl + Pyr) >0.5 was found to water and sediments, indicating a variable impact from urban traffic emissions and biomass burning (Fig. 4a). Ratio BaA/(BaA + Chr) >0.35 was found in water and in sediments, which suggests vehicular emissions (Fig. 4b); and a similar behavior was observed for ratio InP/(InP + BghiP), which indicated combustion sources (Fig. 4b). Moreover, the BbF/BkF ratio was between 1.4 (in SPM) and 1.8 (in sediment), similar to the range reported in literature for wood burning and automobile emissions (Patrolecco et al., 2010). Finally, the LMW/HMW ratio was <1 for most sites, suggesting a pyrolytic origin of PAHs at these sites (mean 0.82; range 0.10–5.80).

These results, obtained by different molecular ratios, were correlated with the specific pollution conditions in the Tiber River catchment. The Tiber River drainage basin passes through large industrial cities in central Italy, that contain steel mills, such as the city of Terni, chemical plants and paper mills; and large agricultural areas. The emission of atmospheric particles from factories and from intensive agricultural activities, also cause serious air pollution, and the particulate-associated PAHs may transport and deposit into the river. In addition to these inputs, the municipal wastewater and vehicular emission from densely populated urban area of Rome, result in the pattern of pyrolytic origins of selected PAHs contamination in the area.

Furthermore to pyrolytic and petrogenic sources, Per is also produced through in situ degradation of biogenic precursors (Baumard et al., 1998; Tobiszewski and Namiesnik, 2012; Pérez-Fernández et al., 2015; Singare, 2015). Indeed, Per is probably the most important diagenetic PAH encountered in sedimentary environments and, thus, a high abundance of Per relative to other PAHs can indicate an important natural origin of PAHs. Per was frequently associated with marine, riverine and estuarine inputs and its concentrations above 10% of the total penta-aromatic isomers indicate a probable diagenetic input, while those in which Per accounts for less than 10% indicate a probable pyrolytic origin of the compound (Baumard et al., 1998; Yancheshmeh et al., 2014; Wakeham and Canuel, 2015). In the present study, the Per concentrations detected in all sediment samples were very low (range 0.10–15.3 ng g^{-1}) and contributed less than 5% to the penta-aromatic isomers and less than 3% to the total PAHs (Fig. S2 in the Supplementary material), indicating a pyrolytic origin of these compounds.

In addition to PAH diagnostic ratio, PCA was conducted for the sixteen selected PAHs in 21 water samples (sum of DP and SPM) of four sampling campaigns (Fig. 5). On the first component (Factor 1) all variables coordinates are positive (70.5%) therefore it represents a weighted average of the variables and it is referred to as measure of overall pollution rate. Likewise, the positive and negative coefficients (14.2%) in the second components (Factor 2) may be regarded as an indication of the probable PAHs source (pyrolytic vs petrogenic). The plot of the first two or three loadings against each other enhances visual interpretation. These results confirmed that the prevailing PAHs source in the Tiber River and Estuary was pyrolytic.

3.6. Ecological risk assessment

In order to assess the ecological toxicity of individual PAHs in sediments, two sets of Sediment quality guidelines (SQGs), including ERL/ERM and TEL/PEL values, were applied (Long et al., 1995; MacDonald et al., 1996). These two sets of SQGs are defined as: i) effect range low (ERL)/effect range median (ERM) and ii) the threshold effect level (TEL)/probable effect level (PEL). ERLs and TELs represent chemical concentrations below which the probability of toxicity and other effects are rare. Differently, the ERMs and PELs represent mid-range above which adverse effects would occur frequently. ERLs-ERMs and TELs-PELs represent a possible-effects range, within which negative effects would occasionally occur (Di Leonardo et al., 2014; Li et al., 2015a; Wang et al., 2015b; Adeleye et al., 2016). In the Tiber River, the total PAH concentrations in sediment samples were below the TEL and ERL values and significantly lower than the PEL and ERM values (Table 3). In relation to the individual compounds, the mean concentrations of detected PAHs were lower than their respective PEL values, while TEL values were exceeded for Acy in 29%, for Ace in 24%, for Flu in 5% and for DahA in 86% of all samples, suggesting that adverse biological effect might occasionally occur. The concentrations of individual PAHs did not exceed their respective ERM values, but exceed the ERL values for Flu in 5% and for DahA in 10%. The results indicated that certain sites may have individual PAHs that occasionally cause biological impairment, nevertheless the ecosystem risk of PAHs in the sediments from the Tiber River and Estuary was low.

Many countries have developed Environmental Quality Standards (EQS) for priority substances and other pollutants in surface and coastal waters. Although compliance with EC-EQS (Directive 2008/105/EC, 2008) in surface waters is checked using an annual average of monthly whole water (dissolved + SPM) concentrations, our data showed that the mean values of BaP and BkF + BbF concentration in the River Tiber (12.2 and 24.8 ng L^{-1}, respectively) were lower than the EC-EQS values (50 and 30 ng L^{-1}, respectively), while mean value of BghiP + InP values (34.8 ng L^{-1}) was significantly higher than the EC-EQS value of 2 ng L^{-1}, showing that the ecological integrity of the river watercourse is possibly at risk.

The toxicity assessment of sediments from Tiber River and its Estuary was carried out according to the total concentration of the seven carcinogenic PAHs. The sum concentrations of these carcinogenic PAHs in

sediment samples ranged from 16.3 ng g^{-1} to 357.9 ng g^{-1}, with a mean value of 94.4 ng g^{-1}, accounting for 49.7% of the total concentration of PAHs. The total TEQ_{PAHs} values calculated for sediment samples varied from 7.05 ngTEQ g^{-1} to 174.4 ngTEQ g^{-1} d.w., with an average of 45.3 ngTEQ g^{-1} d.w. The maximum total TEQ_{PAHs} value was found at site 1 (Fig. 6). The average level of total TEQ_{PAHs} found in sediment samples of the Tiber River and its Estuary was lower than in the sediments of Bahia Blanca, Argentina (Oliva et al., 2015) and in the sediments of Loire River, France (Bertrand et al., 2015); but were similar to those found in in the sediments of Mithi River, India (Singare, 2015) and the sediments of Cauca River, Colombia (Sarria-Villa et al., 2016). This showed that TEQ_{PAHs} values of the Tiber River and its Estuary were in a low level and indicates that less ecological risk exists in the Tiber River basin.

4. Conclusions

This study provided important data on the occurrence, distribution and probable sources of PAHs in the Tiber River and its input into the Tyrrhenian Sea (Central Mediterranean Sea). The levels of PAH concentrations in DP, SPM and sediment phases varied significantly among sampling locations. Two and three-ring PAHs were abundant in water samples, whereas, high molecular weight PAHs were major species in sediment samples. The derived individual diagnostic PAHs ratio and PCA indicated that the PAHs mainly had a pyrolytic source and suggest that important contribution for this pollution derive mainly from combustion processes and vehicle traffic. In relation to the ecotoxicological assessment, although concentrations of several individual PAHs in some stations were above ERL and/or TEL (and below ERM and/or PEL), which would occasionally cause negative ecological effects, the toxic equivalent concentrations (TEQ) of carcinogenic PAHs suggested that the ecological risk of multiple PAHs was quite low. The results of potential toxicity and biological effect assessment indicated that the surface sediments of the Tiber River and its estuary have low ecological risk and a low probability of toxic pollution. Therefore, the Tiber waters should be routinely monitored since PAHs may cause adverse effect on aquatic ecosystems and organisms.

Acknowledgments

This research received no specific grant from any funding agency in the public, commercial, or not-for-profit sectors.

Appendix A. Supplementary data

Supplementary data to this article can be found online at http://dx.doi.org/10.1016/j.scitotenv.2016.05.183.

References

Acquavita, A., Falomo, J., Predonzani, S., Tamberlich, F., Bettoso, N., Mattassi, G., 2014. The PAH level, distribution and composition in surface sediments from a Mediterranean lagoon: the Marano and Grado Lagoon (Northern Adriatic Sea, Italy). Mar. Pollut. Bull. 81 (1), 234–241. http://dx.doi.org/10.1016/j.marpolbul.2014.01.041.

Adeleye, A.O., Jin, H., Di, Y., Li, D., Chen, J., Ye, Y., 2016. Distribution and ecological risk of organic pollutants in the sediments and seafood of Yangtze Estuary and Hangzhou Bay, East China Sea. Sci. Total Environ. 541, 1540–1548. http://dx.doi.org/10.1016/j.scitotenv.2015.09.124.

Bai, Y., Meng, W., Xu, J., Zhang, Y., Guo, C., Lv, J., Wan, J., 2014. Occurrence, distribution, environmental risk assessment and source apportionment of polycyclic aromatic hydrocarbons (PAHs) in water and sediments of the Liaohe River Basin, China. Bull. Environ. Contam. Toxicol. 93 (6), 744–751. http://dx.doi.org/10.1007/s00128-014-1390-7.

Bajt, O., 2014. Aliphatic and polycyclic aromatic hydrocarbons in Gulf of Trieste sediments (northern Adriatic): potential impacts of maritime traffic. Bull. Environ. Contam. Toxicol. 93 (3), 299–305. http://dx.doi.org/10.1007/s00128-014-1321-7.

Baker, J.E., Eisenreich, S.J., Eadie, B.J., 1991. Sediment trap fluxes and benthic recycling of organic carbon, polycyclic aromatic hydrocarbons, and polychlorobiphenyl congeners in Lake Superior. Environ. Sci. Technol. 25 (3), 500–509.

Baumard, P., Budzinski, H., Michon, Q., Garrigues, P., Burgeot, T., Bellocq, J., 1998. Origin and bioavailability of PAHs in the Mediterranean Sea from mussel and sediment records. Estuar. Coast. Shelf Sci. 47, 77–90.

Bebianno, M.J., Pereira, C.G., Rey, F., Cravo, A., Duarte, D., D'Errico, G., Regoli, F., 2015. Integrated approach to assess ecosystem health in harbor areas. Sci. Total Environ. 514, 92–107. http://dx.doi.org/10.1016/j.scitotenv.2015.01.050.

Berrojalbiz, N., Dachs, J., Ojeda, M.J., Valle, M.C., Castro-Jiménez, J., Wollgast, J., Ghiani, M., Hanke, G., Zaldivar, J.M., 2011. Biogeochemical and physical controls on concentrations of polycyclic aromatic hydrocarbons in water and plankton of the Mediterranean and Black Seas. Glob. Biogeochem. Cycles 25 (4), GB4003. http://dx.doi.org/10.1029/2010GB003775.

Bertrand, O., Mondamert, L., Grosbois, C., Dhivert, E., Bourrain, X., Labanowski, J., Desmet, M., 2015. Storage and source of polycyclic aromatic hydrocarbons in sediments downstream of a major coal district in France. Environ. Pollut. 207, 329–340. http://dx.doi.org/10.1016/j.envpol.2015.09.028.

Bettinetti, R., Galassi, S., Quadroni, S., Volta, P., Capoccioni, F., Ciccotti, E., De Leo, G.A., 2011. Use of *Anguilla anguilla* for biomonitoring persistent organic pollutants (POPs) in brackish and riverine waters in Central and Southern Italy. Water Air Soil Pollut. 217 (1–4), 321–331. http://dx.doi.org/10.1007/s11270-010-0590-y.

Cabrerizo, A., Dachs, J., Moeckel, C., Ojeda, M.J., Caballero, G., Barceló, D., Jones, K.C., 2011. Ubiquitous net volatilization of polycyclic aromatic hydrocarbons from soils and parameters influencing their soil-air partitioning. Environ. Sci. Technol. 45 (11), 4740–4747. http://dx.doi.org/10.1021/es104131f.

Cavalcante, R.M., Sousa, F.W., Nascimento, R.F., Silveira, E.R., Freire, G.S., 2009. The impact of urbanization on tropical mangroves (Fortaleza, Brazil): evidence from PAH distribution in sediments. J. Environ. Manag. 91 (2), 328–335. http://dx.doi.org/10.1016/j.jenvman.2009.08.020.

Cirillo, T., Montuori, P., Mainardi, P., Russo, I., Triassi, M., Amodio-Cocchieri, R., 2006. Multipathway polycyclic aromatic hydrocarbon and pyrene exposure among children living in Campania (Italy). J. Environ. Sci. Health, Part A: Tox. Hazard. Subst. Environ. Eng. 41 (10), 2089–2107.

Deng, H., Peng, P., Huang, W., Song, J., 2006. Distribution and loadings of polycyclic aromatic hydrocarbons in the Xijiang River in Guangdong, South China. Chemosphere 64, 1401–1411.

Deng, G., Yang, W., Zhou, G., Li, Y., Liu, S., 2014. Heavy metals and polycyclic aromatic hydrocarbons in sediments from the Shenzhen River, South China. Environ. Sci. Pollut. Res. Int. 21 (18), 10594–10600. http://dx.doi.org/10.1007/s11356-014-2995-4.

di Lascio, A., Rossi, L., Carlino, P., Calizza, E., Rossi, D., Costantini, M.L., 2013. Stable isotope variation in macroinvertebrates indicates anthropogenic disturbance along an urban stretch of the river Tiber (Rome, Italy). Ecol. Indic. 28, 107–114. http://dx.doi.org/10.1016/j.ecolind.2012.04.006.

Di Leonardo, R., Mazzola, A., Tramati, C.D., Vaccaro, A., Vizzini, S., 2014. Highly contaminated areas as sources of pollution for adjoining ecosystems: the case of Augusta Bay (Central Mediterranean). Mar. Pollut. Bull. 89 (1–2), 417–426. http://dx.doi.org/10.1016/j.marpolbul.2014.10.023.

Directive 2008/105/EC of the European Parliament and of the Council of 16 December 2008 on environmental quality standards in the field of water policy, amending and subsequently repealing Council Directives 82/176/EEC, 83/513/EEC, 84/156/EEC, 84/491/EEC, 86/280/EEC and amending Directive 2000/60/EC of the European Parliament and of the Council. Off. J. Eur. Union 348, 84–97.

Dudhagara, D.R., Rajpara, R.K., Bhatt, J.K., Gosai, H.B., Sachaniya, B.K., Dave, B.P., 2016. Distribution, sources and ecological risk assessment of PAHs in historically contaminated surface sediments at Bhavnagar coast, Gujarat, India. Environ. Pollut. 213, 338–346. http://dx.doi.org/10.1016/j.envpol.2016.02.030.

Ekpo, B.O., Oyo-Ita, O.E., Oros, D.R., Simoneit, B.R., 2012. Distributions and sources of polycyclic aromatic hydrocarbons in surface sediments from the Cross River estuary, S.E. Niger Delta, Nigeria. Environ. Monit. Assess. 184 (2), 1037–1047. http://dx.doi.org/10.1007/s10661-011-2019-5.

Foster, K.L., Stern, G.A., Carrie, J., Bailey, J.N., Outridge, P.M., Sanei, H., Macdonald, R.W., 2015. Spatial, temporal, and source variations of hydrocarbons in marine sediments from Baffin Bay, Eastern Canadian Arctic. Sci. Total Environ. 506-507, 430–443. http://dx.doi.org/10.1016/j.scitotenv. 2014.11.002.

Galarneau, E., 2008. Source specificity and atmospheric processing of airborne PAHs: implications for source apportionment. Atmos. Environ. 42, 8139–8149. http://dx.doi.org/10.1016/j.atmosenv.2008.07.025.

Guigue, C., Tedetti, M., Ferretto, N., Garcia, N., Méjanelle, L., Goutx, M., 2014. Spatial and seasonal variabilities of dissolved hydrocarbons in surface waters from the Northwestern Mediterranean Sea: results from one year intensive sampling. Sci. Total Environ. 466-467, 650–662. http://dx.doi.org/10.1016/j.scitotenv.2013.07.082.

Guo, W., He, M., Yang, Z., Lin, C., Quan, X., Men, B., 2009. Distribution, partitioning and sources of polycyclic aromatic hydrocarbons in Daliao River water system in dry season China. J. Hazard. Mater. 164, 1379–1385. http://dx.doi.org/10.1016/j.jhazmat.2008.09.083.

HELCOM, 1993. Second Baltic Sea pollution load compilation. Baltic Sea Environment Proceedings No. 45, Baltic Marine Environment Protection Commission. Helsinki, Finland.

ISTAT, 2010. 6° censimento nazionale dell'agricoltura. Istituto Nazionale di Statistica. (Available at 02/02/2016 to:) http://censimentoagricoltura.istat.it.

ISTAT, 2014. National Institute of Statistics, Population Housing Census. (Available:) http://dati.istat.it/.

Kanzari, F., Syakti, A.D., Asia, L., Malleret, L., Piram, A., Mille, G., Doumenq, P., 2014. Distributions and sources of persistent organic pollutants (aliphatic hydrocarbons, PAHs, PCBs and pesticides) in surface sediments of an industrialized urban river (Huveaune), France. Sci. Total Environ. 478, 141–151. http://dx.doi.org/10.1016/j.scitotenv.2014.01.065.

Kanzari, F., Asia, L., Syakti, A.D., Piram, A., Malleret, L., Mille, G., Doumenq, P., 2015. Distribution and risk assessment of hydrocarbons (aliphatic and PAHs), polychlorinated

biphenyls (PCBs), and pesticides in surface sediments from an agricultural river (Durance) and an industrialized urban lagoon (Berre lagoon), France. Environ. Monit. Assess. 187 (9), 591. http://dx.doi.org/10.1007/s10661-015-4823-9.
Katsoyiannis, A., Terzi, E., Cai, Q.Y., 2007. On the use of PAH molecular diagnostic ratios in sewage sludge for the understanding of the PAH sources. Is this use appropriate? Chemosphere 69, 1337–1339. http://dx.doi.org/10.1016/j.chemosphere.2007.05.084.
Legambiente, 2006. Monitoraggio sull'illegalità e sullo stato di salute dei fiumi italiani. (Available:) http://www.legambiente.it/contenuti/dossier/fiumi-e-legalit%C3%A0.
León, V.M., García, I., Martínez-Gómez, C., Campillo, J.A., Benedicto, J., 2014. Heterogeneous distribution of polycyclic aromatic hydrocarbons in surface sediments and red mullet along the Spanish Mediterranean coast. Mar. Pollut. Bull. 87 (1–2), 352–363. http://dx.doi.org/10.1016/j.marpolbul. 2014.07.049.
Lewis, M.A., Russell, M.J., 2015. Contaminant profiles for surface water, sediment, flora and fauna associated with the mangrove fringe along middle and lower eastern Tampa Bay. Mar. Pollut. Bull. 95 (1), 273–282. http://dx.doi.org/10.1016/j.marpolbul.2015.04.001.
Li, G., Xia, X., Yang, Z., Wang, R., Voulvoulis, N., 2006. Distribution and sources of polycyclic aromatic hydrocarbons in the middle and lower reaches of the Yellow River, China. Environ. Pollut. 144 (3), 985–993. http://dx.doi.org/10.1016/j.envpol.2006.01.047.
Li, J., Dong, H., Zhang, D., Han, B., Zhu, C., Liu, S., Liu, X., Ma, Q., Li, X., 2015a. Sources and ecological risk assessment of PAHs in surface sediments from Bohai Sea and northern part of the Yellow Sea, China. Mar. Pollut. Bull. 96 (1–2), 485–490. http://dx.doi.org/10.1016/j.marpolbul.2015.05.002.
Li, P., Xue, R., Wang, Y., Zhang, R., Zhang, G., 2015b. Influence of anthropogenic activities on PAHs in sediments in a significant gulf of low-latitude developing regions, the Beibu Gulf, South China Sea: distribution, sources, inventory and probability risk. Mar. Pollut. Bull. 90 (1–2), 218–226. http://dx.doi.org/10.1016/j.marpolbul.2014.10.048.
Lima, A.L.C., Farrington, J.W., Reddy, C.M., 2005. Combustion-derived polycyclic aromatic hydrocarbons in the environment—a review. Environ. Forensic 6, 109–131. http://dx.doi.org/10.1080/15275920590952739.
Lipiatou, E., Tolosa, I., Simó, R., Bouloubassi, I., Dachs, J., Marti, S., Sicre, M.A., Bayona, J.M., Grimalt, J.O., Saliot, A., Albaiges, J., 1997. Mass budget and dynamics of polycyclic aromatic hydrocarbons in the Mediterranean Sea. Deep Sea Res., Part II 44 (3–4), 881–905. http://dx.doi.org/10.1016/S0967-0645(96)00093-8.
Liu, Y., Beckingham, B., Ruegner, H., Li, Z., Ma, L., Schwientek, M., Xie, H., Zhao, J., Grathwohl, P., 2013. Comparison of sedimentary PAHs in the rivers of Ammer (Germany) and Liangtan (China): differences between early- and newly-industrialized countries. Environ. Sci. Technol. 47 (2), 701–709. http://dx.doi.org/10.1021/es3031566.
Liu, Z., He, L., Lu, Y., Su, J., Song, H., Zeng, X., Yu, Z., 2015. Distribution, source, and ecological risk assessment of polycyclic aromatic hydrocarbons (PAHs) in surface sediments from the Hun River, northeast China. Environ. Monit. Assess. 187 (5), 290. http://dx.doi.org/10.1007/s10661-015-4525-3.
Long, E.R., MacDonald, D.D., Smith, S.L., Calder, E.D., 1995. Incidence of adverse biological effects within ranges of chemical concentrations in marine and estuarine sediments. Environ. Manag. 19, 81–97.
Lv, J., Xu, J., Guo, C., Zhang, Y., Bai, Y., Meng, W., 2014. Spatial and temporal distribution of polycyclic aromatic hydrocarbons (PAHs) in surface water from Liaohe River Basin, northeast China. Environ. Sci. Pollut. Res. Int. 21 (11), 7088–7096. http://dx.doi.org/10.1007/s11356-014-2604-6.
Ma, W.L., Liu, L.Y., Qi, H., Zhang, Z.F., Song, W.W., Shen, J.M., Chen, Z.L., Ren, N.Q., Grabuski, J., Li, Y.F., 2013. Polycyclic aromatic hydrocarbons in water, sediment and soil of the Songhua River Basin, China. Environ. Monit. Assess. 185 (10), 8399–8409. http://dx.doi.org/10.1007/s10661-013-3182-7.
MacDonald, D.D., Carr, R.S., Calder, F.D., Long, E.R., 1996. Development and evaluation of sediment quality guidelines for Florida coastal waters. Ecotoxicology 5, 253–278.
Malik, A., Verma, P., Singh, A.K., Singh, K.P., 2011. Distribution of polycyclic aromatic hydrocarbons in water and bed sediments of the Gomti River, India. Environ. Monit. Assess. 172 (1–4), 529–545. http://dx.doi.org/10.1007/s10661-010-1352-4.
Minissi, S., Caccese, D., Passafiume, F., Grella, A., Eleonora, C., Rizzoni, M., 1998. Mutagenicity (micronucleus test in *Vicia faba* root tips), polycyclic aromatic hydrocarbons and heavy metal content of sediments collected in Tiber river and its tributaries within the urban area of Rome. Mutat. Res. 420 (1–3), 77–84. http://dx.doi.org/10.1016/S1383-5718(98)00142-9.
Moeckel, C., Monteith, D.T., Llewellyn, N.R., Henrys, P.A., Pereira, M.G., 2013. Relationship between the concentrations of dissolved organic matter and polycyclic aromatic hydrocarbons in a typical U.K. upland stream. Environ. Sci. Technol. 48 (1), 130–138. http://dx.doi.org/10.1021/es403707q.
Montuori, P., Triassi, M., 2012. Polycyclic aromatic hydrocarbons loads into the Mediterranean Sea: estimate of Sarno River inputs. Mar. Pollut. Bull. 64 (3), 512–520. http://dx.doi.org/10.1016/j.marpolbul.2012.01.003.
Mozeto, A.A., Yamada, T.M., De Morais, C.R., Do Nascimento, M.R., Fadini, P.S., Torres, R.J., Sueitt, A.P., De Faria, B.M., 2014. Assessment of organic and inorganic contaminants in sediments of an urban tropical eutrophic reservoir. Environ. Monit. Assess. 186 (2), 815–834. http://dx.doi.org/10.1007/s10661-013-3419-5.
Mzoughi, N., Chouba, L., 2011. Distribution and partitioning of aliphatic hydrocarbons and polycyclic aromatic hydrocarbons between water, suspended particulate matter, and sediment in harbours of the west coastal of the Gulf of Tunis (Tunisia). J. Environ. Monit. 13 (3), 689–698. http://dx.doi.org/10.1039/c0em00616e.
Nagy, A.S., Szabó, J., Vass, I., 2014. Occurrence and distribution of polycyclic aromatic hydrocarbons in surface water and sediments of the Danube River and its tributaries, Hungary. J. Environ. Sci. Health A Tox. Hazard. Subst. Environ. Eng. 49 (10), 1134–1141. http://dx.doi.org/10.1080/10934529.2014.897155.
Nisbet, I.C., LaGoy, P.K., 1992. Toxic equivalency factors (TEFs) for polycyclic aromatic hydrocarbons (PAHs). Regul. Toxicol. Pharmacol. 16 (3), 290–300.
Oliva, A.L., Quintas, P.Y., La Colla, N.S., Arias, A.H., Marcovecchio, J.E., 2015. Distribution, sources, and potential ecotoxicological risk of polycyclic aromatic hydrocarbons in surface sediments from Bahía Blanca Estuary, Argentina. Arch. Environ. Contam. Toxicol. 69 (2), 163–172. http://dx.doi.org/10.1007/s00244-015-0169-0.
Patrolecco, L., Ademollo, N., Capri, S., Pagnotta, R., Polesello, S., 2010. Occurrence of priority hazardous PAHs in water, suspended particulate matter, sediment and common eels (*Anguilla anguilla*) in the urban stretch of the River Tiber (Italy). Chemosphere 81 (11), 1386–1392. http://dx.doi.org/10.1016/j.chemosphere.2010.09.027.
Patrolecco, L., Capri, S., Ademollo, N., 2015. Occurrence of selected pharmaceuticals in the principal sewage treatment plants in Rome (Italy) and in the receiving surface waters. Environ. Sci. Pollut. Res. Int. 22 (8), 5864–5876. http://dx.doi.org/10.1007/s11356-014-3765-z.
Pérez-Fernández, B., Viñas, L., Franco, M.Á., Bargiela, J., 2015. PAHs in the Ría de Arousa (NW Spain): a consideration of PAHs sources and abundance. Mar. Pollut. Bull. 95 (1), 155–165. http://dx.doi.org/10.1016/j.marpolbul.2015.04.028.
Perra, G., Pozo, K., Guerranti, C., Lazzeri, D., Volpi, V., Corsolini, S., Focardi, S., 2011. Levels and spatial distribution of polycyclic aromatic hydrocarbons (PAHs) in superficial sediment from 15 Italian marine protected areas (MPA). Mar. Pollut. Bull. 62 (4), 874–877. http://dx.doi.org/10.1016/j.marpolbul.2011.01.023.
Santana, J.L., Massone, C.G., Valdés, M., Vazquez, R., Lima, L.A., Olivares-Rieumont, S., 2015. Occurrence and source appraisal of polycyclic aromatic hydrocarbons (pahs) in surface waters of the Almendares River, Cuba. Arch. Environ. Contam. Toxicol. 69 (2), 143–152. http://dx.doi.org/10.1007/s00244-015-0136-9.
Sarria-Villa, R., Ocampo-Duque, W., Páez, M., Schuhmacher, M., 2016. Presence of PAHs in water and sediments of the Colombian Cauca River during heavy rain episodes, and implications for risk assessment. Sci. Total Environ. 540, 455–465. http://dx.doi.org/10.1016/j.scitotenv.2015.07.020.
Siemers, A.K., Mänz, J.S., Palm, W.U., Ruck, W.K., 2015. Development and application of a simultaneous SPE-method for polycyclic aromatic hydrocarbons (PAHs), alkylated PAHs, heterocyclic PAHs (NSO-HET) and phenols in aqueous samples from German rivers and the North Sea. Chemosphere 122, 105–114. http://dx.doi.org/10.1016/j.chemosphere.2014.11.022.
Singare, P.U., 2015. Studies on polycyclic aromatic hydrocarbons in surface sediments of Mithi River near Mumbai, India: assessment of sources, toxicity risk and biological impact. Mar. Pollut. Bull. 101 (1), 232–242. http://dx.doi.org/10.1016/j.marpolbul.2015.09.057.
Song, X., Hu, X., He, M., Liang, R., Li, Y., Li, F., 2013. Distribution and sources of polycyclic aromatic hydrocarbons in the surface water of Taizi River, Northeast of China. Environ. Monit. Assess. 185, 8375–8382. http://dx.doi.org/10.1007/s10661-013-3179-2.
Steen, R.J.C.A., van der Baart, M., Hiep, B., van Hattum, W.P., Cono, W.P., Brinkman, U.A.T., 2001. Gross fluxes and estuarine behaviour of pesticides in the Scheldt estuary (1995–1997). Environ. Pollut. 115, 65–79. http://dx.doi.org/10.1016/S0269-7491(01)00085-9.
Sun, J.H., Wang, G.L., Chai, Y., Zhang, G., Li, J., Feng, J., 2009. Distribution of polycyclic aromatic hydrocarbons (PAHs) in Henan Reach of the Yellow River, Middle China. Ecotoxicol. Environ. Saf. 72, 1614–1624.
Tavakoly Sany, S.B., Hashim, R., Salleh, A., Rezayi, M., Mehdinia, A., Safari, O., 2014. Polycyclic aromatic hydrocarbons in coastal sediment of klang strait, Malaysia: distribution pattern, risk assessment and sources. PLoS One 9 (4), e94907. http://dx.doi.org/10.1371/journal.pone.0094907.
Tobiszewski, M., Namiesnik, J., 2012. Review – PAH diagnostic ratios for the identification of pollution emission sources. Environ. Pollut. 162, 110–119.
Tuncel, S.G., Topal, T., 2015. Polycyclic aromatic hydrocarbons (PAHs) in sea sediments of the Turkish Mediterranean coast, composition and sources. Environ. Sci. Pollut. Res. Int. 22 (6), 4213–4221. http://dx.doi.org/10.1007/s11356-014-3621-1.
UNEP/MAP, 2004. Guidelines for river (including estuaries) pollution monitoring programme for the Mediterranean region. MAP Technical Reports Series No. 151. UNEP/MAP, Athens.
USEPA, 2012. (US Environmental Protection Agency). Regional screening levels for chemical contaminants at superfund sites. Regional Screening Table. User's Guide (Available at 15/12/2015 to: http://www.epa.gov/risk/regional-screening-table-users-guide-november-2015).
Wakeham, S.G., Canuel, E.A., 2015. Biogenic polycyclic aromatic hydrocarbons in sediments of the San Joaquin River in California (USA), and current paradigms on their formation. Environ. Sci. Pollut. Res. Int. http://dx.doi.org/10.1007/s11356-015-5402-x.
Walling, D.E., Webb, B.W., 1985. Estimating the discharge of contaminants to coastal waters by rivers: some cautionary comments. Mar. Pollut. Bull. 16, 488–492.
Wang, M., Wang, C., Hu, X., Zhang, H., He, S., Lv, S., 2015a. Distributions and sources of petroleum, aliphatic hydrocarbons and polycyclic aromatic hydrocarbons (PAHs) in surface sediments from Bohai Bay and its adjacent river, China. Mar. Pollut. Bull. 90 (1–2), 88–94. http://dx.doi.org/10.1016/j.marpolbul.2014.11.017.
Wang, Y.B., Liu, C.W., Kao, Y.H., Jang, C.S., 2015b. Characterization and risk assessment of PAH-contaminated river sediment by using advanced multivariate methods. Sci. Total Environ. 524–525, 63–73. http://dx.doi.org/10.1016/j.scitotenv.2015.04.019.
Wilcke, W., 2007. Global patterns of polycyclic aromatic hydrocarbons (PAHs) in soil. Geoderma 141 (3–4), 157–166.
Wu, Y., Wang, X., Li, Y., Ya, M., Luo, H., Hong, H., 2015. Polybrominated diphenyl ethers, organochlorine pesticides, and polycyclic aromatic hydrocarbons in water from the Jiulong River estuary, China: levels, distributions, influencing factors, and risk assessment. Environ. Sci. Pollut. Res. http://dx.doi.org/10.1007/s11356-015-4782-2.
Yancheshmeh, R.A., Bakhtiari, A.R., Mortazavi, S., Savabieasfahani, M., 2014. Sediment PAH: contrasting levels in the Caspian Sea and Anzali Wetland. Mar. Pollut. Bull. 84 (1–2), 391–400. http://dx.doi.org/10.1016/j.marpolbul.2014.05.001.
Yu, W., Liu, R., Xu, F., Shen, Z., 2015. Environmental risk assessments and spatial variations of polycyclic aromatic hydrocarbons in surface sediments in Yangtze River estuary,

China. Mar. Pollut. Bull. 100 (1), 507–515. http://dx.doi.org/10.1016/j.marpolbul.2015.09.004.

Yunker, M.B., Macdonald, R.W., Vingarzan, R., Mitchell, R.H., Goyette, D., Sylvestre, S., 2002. PAHs in the Fraser River basin: a critical appraisal of PAH ratios as indicators of PAH source and composition. Org. Geochem. 33, 489–515.

Zhang, Q., Pei, G., Liu, G., Li, H., Gao, L., 2015. Distribution and photochemistry of polycyclic aromatic hydrocarbons in the Baotou section of the Yellow River during winter. Arch. Environ. Contam. Toxicol. 69 (2), 133–142. http://dx.doi.org/10.1007/s00244-015-0135-x.

Zhao, X., Ding, J., You, H., 2014. Spatial distribution and temporal trends of polycyclic aromatic hydrocarbons (PAHs) in water and sediment from Songhua River, China. Environ. Geochem. Health 36 (1), 131–143. http://dx.doi.org/10.1007/s10653-013-9524-0.

Zhao, X., Qiu, H., Zhao, Y., Shen, J., Chen, Z., Chen, J., 2015. Distribution of polycyclic aromatic hydrocarbons in surface water from the upper reach of the Yellow River, Northwestern China. Environ. Sci. Pollut. Res. Int. 22 (9), 6950–6956. http://dx.doi.org/10.1007/s11356-014-3846-z.

Zheng, B., Wang, L., Lei, K., Nan, B., 2016. Distribution and ecological risk assessment of polycyclic aromatic hydrocarbons in water, suspended particulate matter and sediment from Daliao River estuary and the adjacent area, China. Chemosphere 149, 91–100. http://dx.doi.org/10.1016/j.chemosphere.2016.01.039.

Zhi, H., Zhao, Z., Zhang, L., 2015. The fate of polycyclic aromatic hydrocarbons (PAHs) and organochlorine pesticides (OCPs) in water from Poyang Lake, the largest freshwater lake in China. Chemosphere 119, 1134–1140. http://dx.doi.org/10.1016/j.chemosphere.2014.09.054.